

Article

Dynamic Simulation of Land Use and Habitat Quality Assessment in Baiyangdian Basin Using the SD-PLUS Coupled Model

Zhen Han ^{1,2,3}, Budong Li ^{1,2,3} , Zepeng Han ⁴, Shiyan Wang ^{1,2,3,*}, Wenqi Peng ^{1,2,3}, Xiaobo Liu ^{1,2,3} and David Benson ⁵

- ¹ State Key Laboratory of Simulation and Regulation of Water Cycle in River Basin, China Institute of Water Resources and Hydropower Research, Beijing 100038, China; zhenhan@iwhr.com (Z.H.)
- ² Department of Water Ecology and Environment, China Institute of Water Resources and Hydropower Research, Beijing 100038, China
- ³ Key Laboratory of Water Safety for Beijing-Tianjin-Hebei Region of Ministry of Water Resources, Beijing 100038, China
- ⁴ CSD Water Service, Beijing 100192, China
- ⁵ Environment and Sustainability Institute, Penryn Campus, University of Exeter, Penryn TR10 9FE, UK
- * Correspondence: wangsy@iwhr.com

Abstract: The physical foundation and environmental assurance provided by the regional habitat are crucial for the survival and sustainable development of organisms. Land use change, as a significant manifestation of human activity, is a crucial factor in habitat quality. An SD-PLUS coupled model was developed to simulate land use change in the Baiyangdian (BYD) Basin using data on land use, socio-economic factors, and the climatic environment from 2000 to 2020. The InVEST model was employed to assess the habitat quality of the basin from 2000 to 2050. The findings indicated the following: Between 2020 and 2050, the predominant land use changes across the three scenarios involve the conversion of farmland to construction land and grassland to woodland. The magnitude of these changes steadily declines over time. The magnitude of change in land use for all kinds was greater under SSP5 compared to SSP1 and SSP2. The movement of habitat quality grades primarily occurred from higher grades to lower grades. In 2050, the habitat quality is projected to improve compared to 2020 under three different scenarios. The highest improvement is expected in SSP5 with a 0.60% increase, followed by SSP2 with a 0.42% increase and SSP1 with the smallest increase of 0.23%.

Keywords: land use; scenario simulation; SD-PLUS coupling model; InVEST model; habitat quality; BYD Basin



Citation: Han, Z.; Li, B.; Han, Z.; Wang, S.; Peng, W.; Liu, X.; Benson, D. Dynamic Simulation of Land Use and Habitat Quality Assessment in Baiyangdian Basin Using the SD-PLUS Coupled Model. *Water* **2024**, *16*, 678. <https://doi.org/10.3390/w16050678>

Academic Editor: Salvador García-Ayllón Veintimilla

Received: 22 December 2023

Revised: 3 February 2024

Accepted: 19 February 2024

Published: 26 February 2024



Copyright: © 2024 by the authors. Licensee MDPI, Basel, Switzerland. This article is an open access article distributed under the terms and conditions of the Creative Commons Attribution (CC BY) license (<https://creativecommons.org/licenses/by/4.0/>).

1. Introduction

Habitat quality pertains to the capacity of an ecosystem to offer appropriate living conditions for individuals and populations, serving as a reflection of the overall status of regional biodiversity [1,2]. Human activities have significantly modified the distribution of regional habitats, leading to issues such as habitat fragmentation, degradation, and potential loss [3]. These challenges arise from population growth and rapid economic development, profoundly impacting the circulation of material and energy flow among habitat patches [4]. Land use/cover change (LUCC) emerges as the primary threat to habitat quality [5,6], serving as an indicator of the extent of human activity. Therefore, it is crucial to investigate temporal and geographical variations in LUCC and habitat quality, and understand how they are influenced by human activities to ensure regional ecological security.

Currently, the exploration of a multi-scenario simulation for future LUCC relies on the overarching framework of “scenario establishment-demand prediction-spatial distribution”.

Various models are employed for demand prediction, including system dynamics (SD), Markov chains, and linear programming models. For spatial simulation, common models include cellular automata (CA) [7], the Conversion of Land Use and its Effects modeling framework (CLUE) [8], Future Land Use Simulation (FLUS) [9], and the Patch-generating Land Use Simulation (PLUS) Model [10]. The system dynamics (SD) model is particularly effective in representing the nonlinear, systematic, complicated, and dynamic features of the LUCC process, making it a valuable tool for simulating land use scenarios [11,12]. The FLUS model has demonstrated excellent simulation accuracy compared to classic models such as CLUE-S, ANN-CA, and Logistic-CA [9]. Additionally, the PLUS model exhibits superior spatial fitting when compared to the FLUS model [13,14]. Wang et al. conducted a comparative study in Beijing municipality, evaluating CA-Markov, FLUS, and PLUS models, with their findings indicating that the predictive accuracy of the PLUS model surpasses that of the other two models [15]. He et al. applied the PLUS model to predict LUCC in the Yangtze River Basin, demonstrating accurate simulations and predictions under various scenarios [16]. Another study by Wang et al. involved a dynamic simulation of LUCC at an urban scale using a linked SD model and a PLUS model, supplemented by the InVEST model to analyze carbon stock features in relation to the evolution of LUCC based on climate change scenarios [11]. The combination of the demand prediction model and the spatial simulation model facilitates the integration of their respective benefits, resulting in enhanced simulation accuracy [13]. This diverse set of models provides a comprehensive approach to studying LUCC, with each model contributing unique insights to the understanding of future land use scenarios.

Regarding the assessment of habitat quality in specific regions, numerous researchers have utilized the InVEST model for quantitative investigations, yielding positive outcomes. Huang et al. utilized the InVEST model and topographic location to analyze spatiotemporal changes in habitat quality and the interaction between landscape patterns and gradient effects in Shucheng County. Their findings underscored the significant impact of topography and landscape patterns on habitat quality evolution [17]. In a study assessing habitat quality and deterioration in Italy, Sallustio et al. employed the InVEST software cartographically. They emphasized that habitat quality and degradation are influenced by geographical position and human-induced influences, varying in susceptibility to conservation efforts [18]. Moreira proposed a method for assessing the preservation condition of natural habitats in the Azores, specifically on the island of Pico in Portugal, using the InVEST habitat quality model. The results highlighted notably favorable conditions in ecosystems at high altitudes, attributed to the absence of significant hazards such as invasive alien species and rangelands [19]. In a multi-scenario simulation analysis examining the impact of land use on the quality of human settlements in Tianjin, Li et al. utilized the PLUS model and the InVEST Integrated Valuation of Ecosystem Services and Tradeoffs model. They identified the continuous increase in construction land as the primary factor contributing to the decline in habitat quality over time [20]. Wang et al. conducted a study to analyze the impacts of climate change on the regional ecology of Yunnan Province. Their research involved the use of coupled models, specifically employing the PLUS and InVEST models for simulation and analysis [21]. In a separate study, Babbar et al. utilized the Markov chain and InVEST model to assess and predict carbon sequestration in the Sariska Tiger Reserve [22].

In 2010, the United Nations Intergovernmental Panel on Climate Change (IPCC) introduced Shared Socioeconomic Pathways (SSPs) in conjunction with Representative Concentration Pathways (RCPs). These pathways take into account various socio-economic development factors [23]. The SSPs scenario comprises five socio-economic development models [24], namely the sustainable development path (SSP1), natural development path (SSP2), regional competition path (SSP3), unbalanced path (SSP4), and high-speed development path (SSP5). The utilization of SSPs in conjunction with LUCC simulations enables a comprehensive assessment of the interplay between human activities and ecosystems [25]. Increasingly, researchers have conducted numerous studies to forecast future LUCC by

integrating multiple models. Scenario simulation involves predicting future changes in development modes by making assumptions about the future social economy, population, or climate. It offers a fresh perspective for LUCC research [26].

In April 2017, China established the Xiong'an New Area with the aim of "relocating non-capital functions from Beijing and promoting coordinated development in the Beijing-Tianjin-Hebei (BTH) region". Located in the eastern plain of the BYD basin, the Xiong'an New Area has experienced a significant expansion of construction land as its urbanization process accelerates. This expansion has resulted in the substantial encroachment upon grassland, farmland, and woodland, despite a simultaneous increased national investment in ecological protection. Although efforts have been made to enhance ecological conservation, the region's habitat quality in the BYD basin is still expected to be impacted by changes in land use. Currently, there is limited research focused on the alterations in land use and habitat quality within the BYD basin against the backdrop of the construction and development of the Xiong'an New Area. This study endeavors to simulate the spatiotemporal changes in land use and habitat quality within the BYD basin, examining three distinct development scenarios (SSP1, SSP2, SSP5), with a particular emphasis on SSP5 and SSP1 scenarios. The primary objective of this research is to assess the responses and mechanisms governing habitat quality in BYD amidst policy disturbances and SSP2 scenarios. The findings of this analysis aim to provide valuable insights for the high-quality, sustainable development of both the Xiong'an New Area and the BYD basin, serving as a reference for informed decision-making.

2. Data and Methods

2.1. Study Area

The BYD basin is situated in the central region of the North China Plain, namely between longitudes 113°40' to 116°16' E and latitudes 38°04' to 40°04' N. The BYD Lake is part of the Daqing River system within the Haihe River basin. The administrative division encompasses the BTH region (Figure 1). The cumulative surface area of the basin is approximately 3.12×10^4 km². The topography exhibits elevated features in the northwest, lower features in the southeast, and rugged features in the west. The primary land utilization categories consist of woodland and grassland. The eastern region is characterized by flat terrain, with the primary land use consisting of agricultural land and areas designated for construction. The mountainous areas and plains account for 57.2% and 42.8% of the total area, respectively [27]. The BYD basin features a temperate continental monsoon climate, with an annual precipitation of 556 mm and an annual evaporation of 1637 mm. The average annual temperature in the region varies from 7.3 °C to 12.7 °C [28].

2.2. Data Sources

The relevant data are presented in Table 1. The primary data for the SD model include the SSPs dataset, land use information, socio-economic indicators (such as population, GDP, and fixed asset investment in different industries), and BYD water level data. The PLUS model data consist of raster data representing land use and driving factors. These factors include seven socio-economic variables (GDP, population density, distance from railway, expressways, national highway, provincial highway, and water system) and five climatic and environmental variables. The China land cover dataset (CLCD) in the BYD basin has been classified into six categories based on the current conditions: farmland, woodland, grassland, water, construction land, and unutilized land. The data mentioned above were consolidated in ArcGIS, including the number of rows and columns and the projection coordinate system, and resampling was employed to transform the data into raster format with a resolution of 30 m.

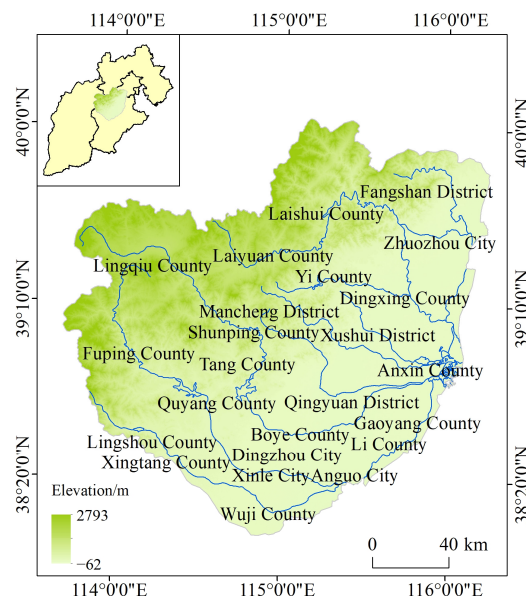


Figure 1. Location of BYD Basin.

Table 1. Details of research data.

Data Type	Name	Time	Attribute	Sources
Scenario	SSPs	2010–2050.	Cell point/0.5°	Jiang Tong et al. [24]
Land Use	CLCD	2000–2020.	Raster/30 m	Yang and Huang [29]
Socio-Economic	GDP	2019	Grid/1 km	Resources and Environmental Science and Data Center (https://www.resdc.cn) China City Statistical Yearbook, Annual Bulletin of Baoding City
	Population density	2020	Grid/1 km	
Climatic Environmental	Statistical Yearbook	2000–2020.	Statistics	
	Average annual temperature	2000–2015.	Grid/1 km	Resources and Environmental Science and Data Center (https://www.resdc.cn)
	Average annual precipitation	2000–2015.	Grid/1 km	
	Soil type	1995	Grid/1 km	Yearbook of Haihe River Basin Hydrological Data Geospatial data Cloud platform (https://www.gscloud.cn) Extracted from elevation data
	Water Level	2006–2019.	Statistics	
Elevation	/	Grid/30 m		
Road, Water System	Slope	/	Raster/30 m	
	Road network	2016	Vector	National Center for Basic Geographic Information (https://www.webmap.cn)
Water System	2015	Vector		

2.3. Models and Methods

2.3.1. LUCC Future Scenario Demand Prediction Based on SD Model

The SD model framework, in conjunction with the data of land use, was developed using Vensim software(v7.3.5) and information from the provinces and localities included in the study area, as well as the China Urban Statistical Yearbook and bulletins on the economy, population, and water level (Figure 2).

The relationship equations between variables were established using the SPSS software (R26.0.0.0), incorporating historical data from 2000 to 2050. In the historical simulation phase covering the period from 2000 to 2020, the accuracy of the research results is evaluated by comparing them with historical data. Upon conducting a thorough analysis of the land use values for the year 2020, it is evident that the relative errors between the actual and simulated data are found to be below 5%, as presented in Table 2. The concentrated distribution of various land use types in the BYD basin, particularly with forested areas predominantly located in the western mountainous region, is responsible for this phenomenon. Additionally, the human activity disturbance is low, contributing to higher model accuracy. This paper focuses on the selection of three scenarios, namely SSP1, SSP2, and SSP5, for

the purpose of predicting future demand. SSP1, also known as Shared Socioeconomic Pathway 1, is distinguished by its moderate to high economic development and relatively low population levels. SSP2 is characterized by a moderate economic level and population size, while SSP5 is characterized by a high economic level and a relatively smaller middle population size [30].

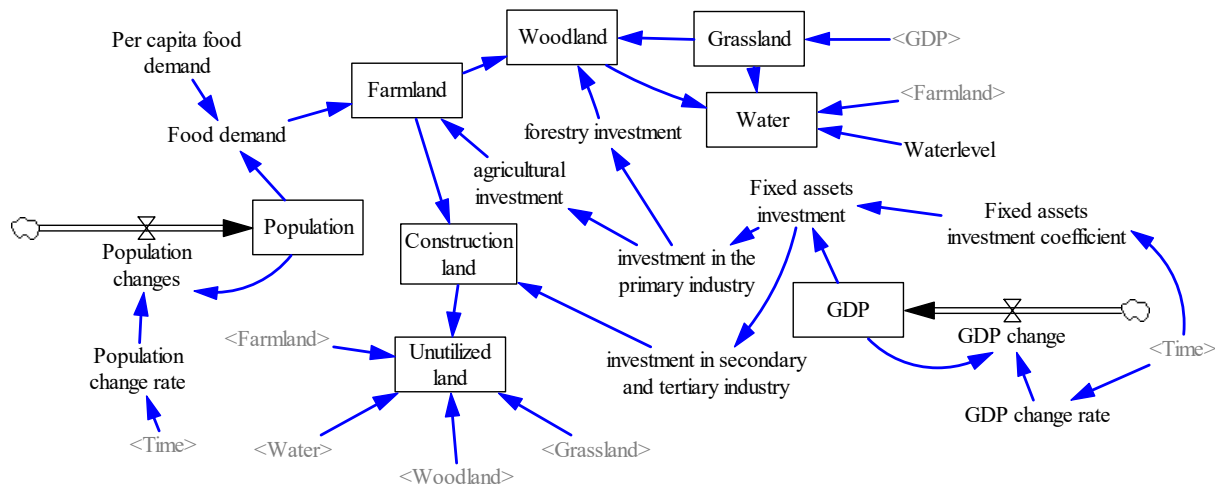


Figure 2. SD model framework.

Table 2. Verification of simulation accuracy of SD model.

Landscape Type	Actual Area in 2020/km ²	Simulated Area in 2020/km ²	Relative Error/%
Farmland	12,675.08	12,428.31	−1.95
Woodland	8484.29	8456.03	−0.33
Grassland	5574.27	5786.59	3.81
Water	169.67	171.00	0.78
Construction land	4322.14	4378.33	1.30

The key factors to consider in future scenario analysis are the economic and population parameters. The population parameters consist of the estimated population data for each province under the universal two-child policy; the economic parameters are the total GDP of each province (2010 price). The average rate of change over a ten-year period is computed for the population parameters. The parameters for various scenarios have been established and are presented in Table 3.

Table 3. Parameter setting for different scenarios.

Variables	2020–2030.			2030–2040.			2040–2050.		
	SSP1	SSP2	SSP5	SSP1	SSP2	SSP5	SSP1	SSP2	SSP5
GDP change rate/%	4.64	4.67	4.59	2.36	2.38	2.61	1.36	1.10	1.81
Population change rate/%	0.91	2.24	1.59	−0.49	0.53	0.31	−2.25	−0.52	−1.41

2.3.2. Introduction of InVEST Model

The Habitat Quality module of the InVEST model can calculate the degree of degradation of habitat quality based on the relationship between land use types and threat factors, and then calculate habitat quality.

The equation used to determine the extent of habitat degradation is as follows:

$$D_{xj} = \sum_{r=1}^R \sum_{y=1}^{Y_r} \left(\frac{w_r}{\sum_{r=1}^R w_r} \right) r_y i_{rxy} \beta_x S_{jr} \tag{1}$$

$$i_{rxy} = \begin{cases} 1 - \left(\frac{d_{xy}}{d_{rmax}}\right) & \text{(Linear recession)} \\ \exp\left[-\left(\frac{2.99}{d_{rmax}}\right) \times d_{xy}\right] & \text{(Exponential recession)} \end{cases} \quad (2)$$

where D_{xj} is the habitat degradation degree of grid x of land use type j ($0 \leq D_{xj} \leq 1$, the greater the value, the higher the habitat degradation degree); r is the habitat threat factor; y is the grid in threat factor r ; w_r is the weights of different threat factors; r_y is the threat factor intensity; i_{rxy} is the influence of threat factor r in grid y on grid x ; β_x is the anti-interference level of habitat; S_{jr} is the relative sensitivity of different habitats to different threat factors; d_{xy} is the distance between grid x and grid y ; and d_{rmax} is the maximum influence distance of threat factor r .

Habitat quality is calculated by:

$$Q_{xj} = H_j \left(1 - \frac{D_{xj}^z}{D_{xj}^z + k^z}\right) \quad (3)$$

where Q_{xj} is the habitat quality of grid x in land use type j ($0 \leq Q_{xj} \leq 1$, the greater the value, the better the habitat quality); H_j is the habitat suitability of land use type j ; z is the normalized constant of 2.5; and k is the half-full sum constant and takes half of D 's maximum _{xj} value.

Based on the current conditions of the study area, the threat factors selected include farmland, construction land, and roads (including railways, expressways, and national and provincial roads). This decision is informed by the InVEST Model Guide [31] and previous studies [6,32,33]. In order to ascertain the pertinent characteristics of the stress factors (Table 4), it is necessary to assess both the habitat suitability and habitat sensitivity (Table 5).

Table 4. Related parameters of threat factors.

Threat Factor	Maximum Impact Distance/km	Weights	Type of Decline
Farmland	4	0.7	Linear
Construction land	8	1	Index
Railways	5	0.6	Linear
Expressways	3	0.6	Linear
National highways	3	0.6	Linear
Provincial roads	2	0.5	Linear

Table 5. Sensitivity of habitat types to threat factors.

Landscape Types	Habitat Suitability	Susceptibility					
		Farmland	Construction Land	Railway	Expressways	National Highways	Provincial Roads
Farmland	0	0	0	0	0	0	0
Woodland	1	0.5	0.7	0.75	0.7	0.7	0.6
Grassland	0.7	0.6	0.65	0.5	0.3	0.3	0.2
Water	1	0.75	0.7	0.75	0.7	0.7	0.6
Construction land	0	0	0	0	0	0	0
Unutilized land	0	0	0	0	0	0	0

3. Results

3.1. Spatial and Temporal Changes of Land Use from 2000 to 2020

The predominant land uses in the BYD Basin are farmland, woodland, grassland, and construction land. These land uses exhibit distinct variations in their spatial distribution, as depicted in Figure 3. The majority of farmland in the study area is concentrated in the

southeastern plain region, comprising almost 40% of the total area. The mountainous area in the northwest contained a mixture of grassland and woodland, primarily concentrated in the middle and western regions, with a predominant presence in the northern portion. The availability of land suitable for construction is primarily concentrated in plain regions, rural areas, and urban centers. Between 2000 and 2020, there were major changes in the land use area in the study area. Specifically, the area of farmland, grassland, and unutilized land were decreased by 1255.93 km², 1042.12 km², and 8.04 km², respectively. The Woodland area experienced a substantial growth of 873.21 km², whereas the construction land area saw a big increase of 1389.66 km². The water area has undergone substantial changes, decreasing from 126.46 km² in 2000 to 106.10 km² in 2010, and subsequently increasing to 169.67 km² in 2020.

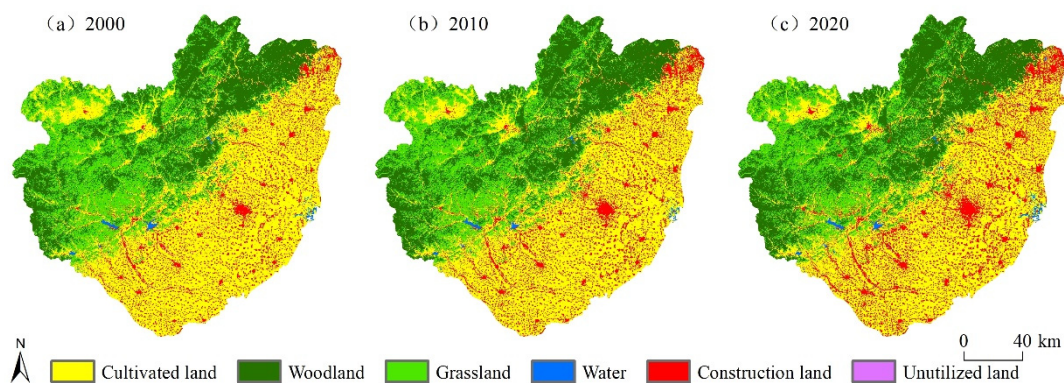


Figure 3. Land use in BYD Basin in 2000, 2010, and 2020.

Figure 4 illustrates that land use transfer primarily encompasses the transfer of farmland and grassland, as well as the transfer of woodland and construction land. A large portion of construction land is converted from farmland, including an area of 1287.13 km². The primary region for this conversion is the southeast plain. Woodland primarily originates from the conversion of farmland and grassland, with the predominant converted area being distributed in a straight line from the northeast to the southwest. The expansion of farmland area primarily results from the conversion of grassland, totaling 487.02 km². The transfer area is primarily situated in the southwestern region, where the mountainous terrain meets the plain area.

3.2. Spatial and Temporal Characteristics of Habitat Quality from 2000 to 2020

The InVEST model was employed for the purpose of quantifying and assessing the habitat quality within the designated study area, spanning the time range of 2000 to 2020. To enhance the examination of temporal and spatial fluctuations in habitat quality, previous research endeavors have been employed to categorize habitat quality into five distinct grades, as depicted in Figure 5. These grades are as follows: In English, the translation would be the following: 0~0.2 is labeled as low, 0.2~0.4 as relatively low, 0.4~0.6 as medium, 0.6~0.8 as relatively high, and 0.8~1 as high [34]. The findings of the study indicate that the average habitat quality values for the years 2010, 2015, and 2020 were observed to be 0.3756, 0.3847, and 0.3836, respectively. In terms of habitat quality, the spatial distribution, particularly in the categories of relatively high and high, primarily encompasses the northwestern mountainous region within the study area. The distribution of low habitat quality was primarily concentrated within the southeastern plain region of the designated study area. The distribution of habitats with relatively low and medium quality was primarily observed in the transitional zone between mountainous and plain regions. From the perspective of time, the period spanning 2000–2020 witnessed the discovery of a substantial proportion, exceeding 50%, of regions characterized by either a relatively low or low habitat quality grade. This observation serves as an indication that the overall state of habitat quality within the designated study area was predominantly low. The spatial distribution

of habitats experienced notable changes during the observed period. Specifically, the areas characterized as high habitats expanded by approximately 827.67 km², whereas the low habitats increased by 118.88 km². Conversely, the relatively low, medium, and high habitats exhibited reductions in their respective areas, with decreases of approximately 97.12 km², 159.61 km², and 689.82 km². These alterations in habitat distribution signify significant shifts in the ecological landscape.

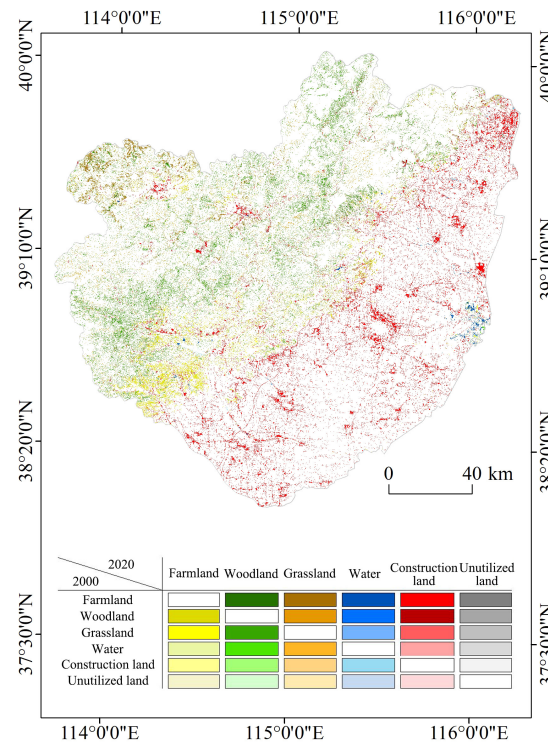


Figure 4. Map of land use type transfer in BYD Basin from 2000 to 2020.

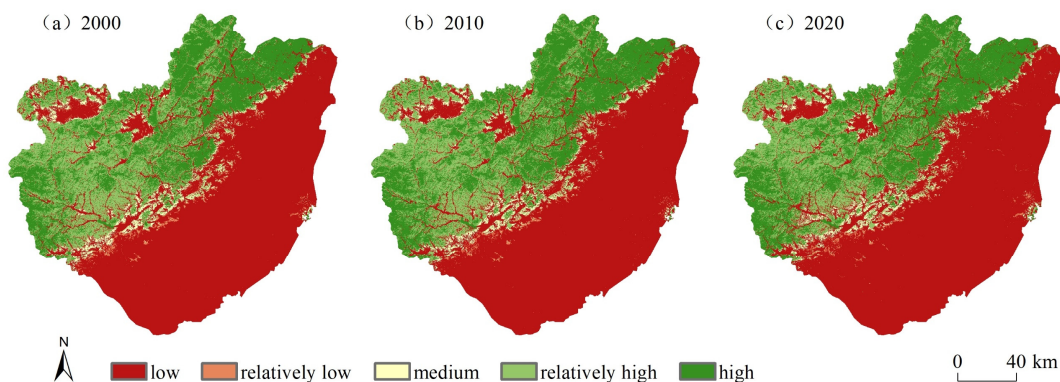


Figure 5. Spatial distribution of habitat quality in BYD Basin from 2000 to 2020.

The LEAS module was employed to assess the extent to which driving factors contribute to changes in habitat quality (Figure 6). The findings indicated that LUCC played a crucial role in contributing to the alteration of habitat quality.

3.3. LUCC Prediction under SSPs Scenario Based on SD-PLUS Coupling Model

The land use demand for SSP1, SSP2, and SSP5 scenarios was determined using the SD model (Figure 7). The spatial-temporal changes in land use under the SSP scenarios were then analyzed using the PLUS model (Figures 8 and 9). The Figure 8 results indicate that between 2020 and 2050, the area of farmland and grassland in the study area exhibits a

declining trend under the SSP1, SSP2, and SSP5 scenarios. Furthermore, the magnitude of the decrease diminishes over time. Specifically, the farmland area exhibits a decrease of 9.28%, 10.22%, and 11.15% under the respective scenarios. The grassland area had a reduction of 8.95%, 10.72%, and 11.71% consecutively. With the passage of time, the amplitude of the upward trend in the area of woodland and construction land diminished. The most significant growth was seen in the area of construction land, which climbed by 20%, 23.12%, and 25.16%, respectively. The area of woodland, on the other hand, increased by 5.19%, 5.59%, and 6.28%, respectively. The water area and unutilized land had an initial increase, followed by a decline, and then another growth. The water area experienced a change of less than 5 km², while the unutilized land area saw a change of less than 0.8 km². However, these changes were not significant or easily noticeable. Figure 9 illustrates that between 2020 and 2050, the land use dynamics in the study area primarily involve the conversion of farmland to construction land and grassland to woodland across the three scenarios of SSP1, SSP2, and SSP5. The land area of farmland to construction land is 1118.10 km², 1233.58 km², and 1350.16 km², while the area of grassland to woodland is 418.31 km², 490.94 km², and 551.32 km², respectively.

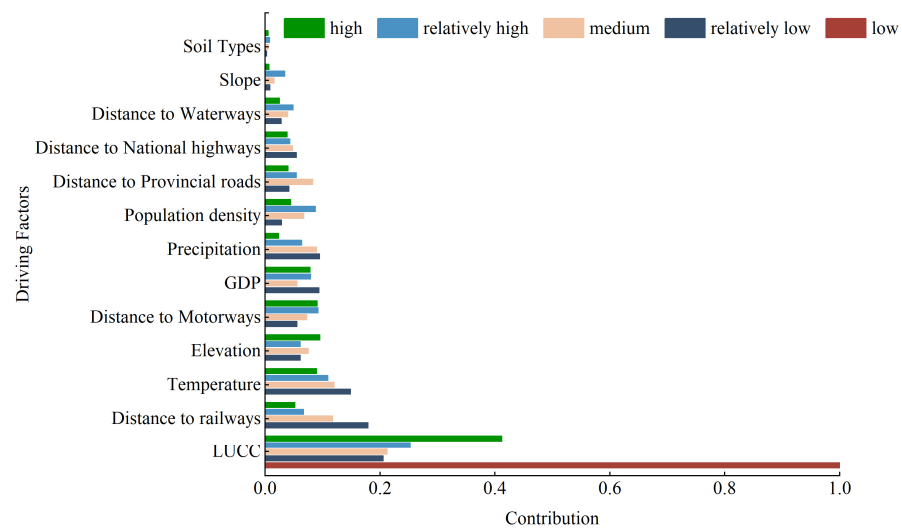


Figure 6. Contribution of drivers to habitat quality.

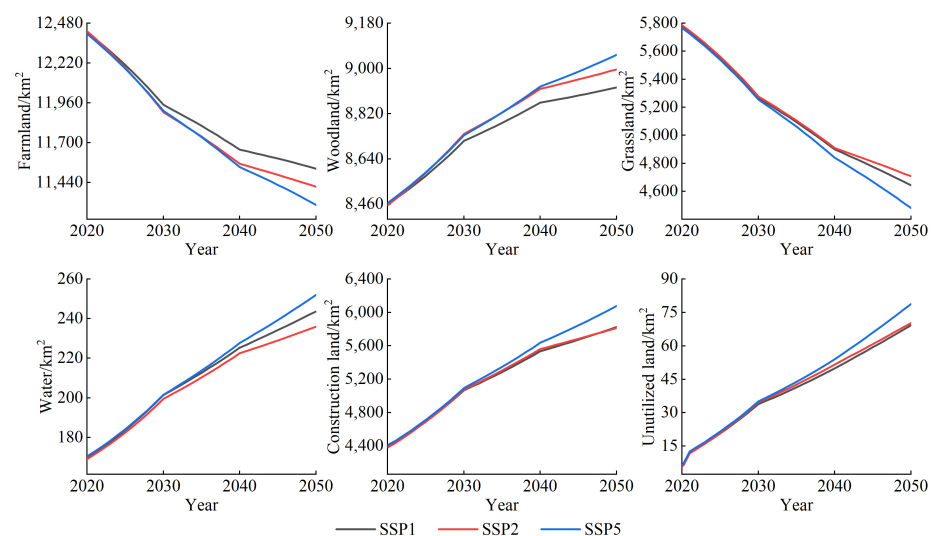


Figure 7. Prediction of land use demand under different SSPs scenarios.

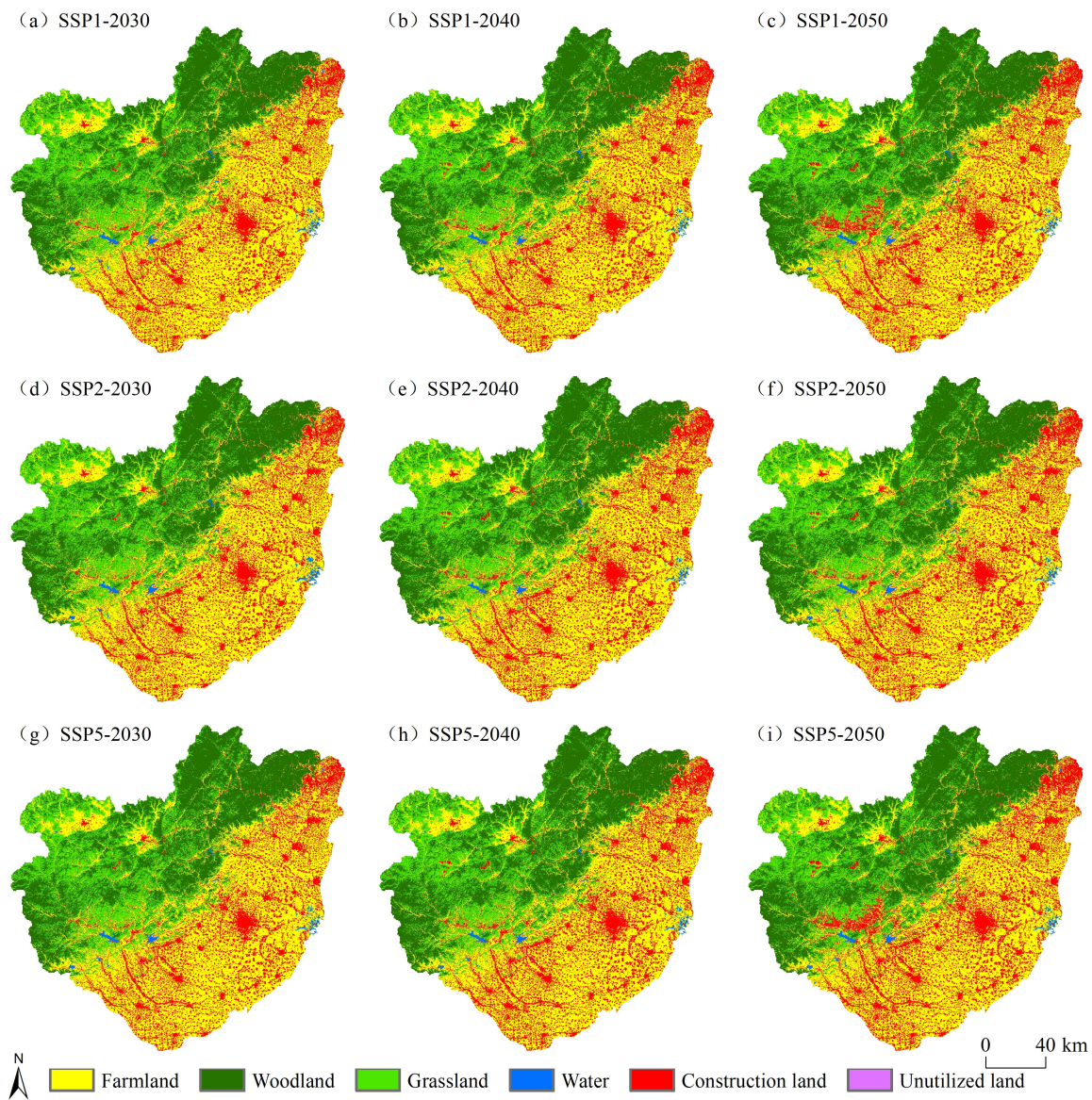


Figure 8. Land use demand in BYD Basin in 2030, 2040, and 2050 under different scenarios.

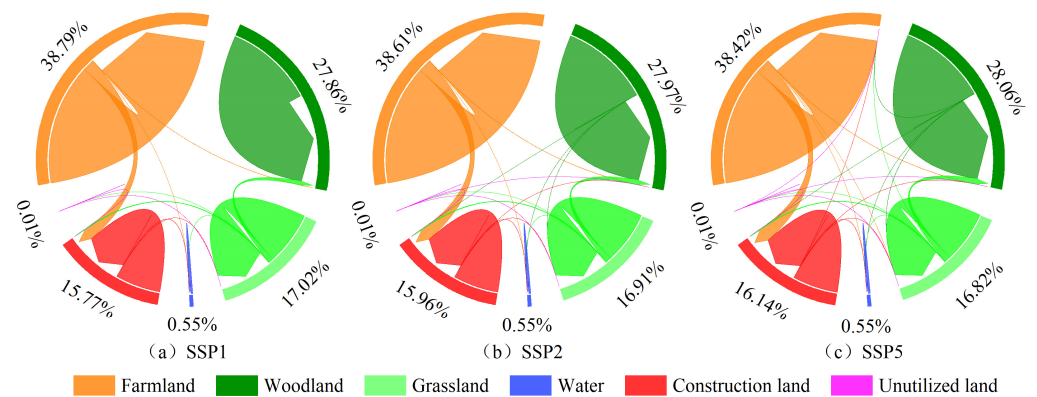


Figure 9. Land use type transfer in BYD Basin in different scenarios from 2020 to 2050.

When comparing LUCC across three scenarios, the findings indicate that the decrease in farmland area is the least significant under the SSP1 scenario, and the rate of growth for building land is the slowest under the SSP1 scenario. The possible reason for this is

that the population is at its minimum in comparison to the other two scenarios, and the amount of arable land converted into construction land is relatively minimal. Furthermore, the conversion of farmland to woodland has the lowest magnitude, with the smallest expansion in the woodland area. Within the SSP2 scenario, the grassland area experienced the smallest reduction, while the shift in construction land closely resembled that of the SSP1 scenario. When comparing the SSP1 and SSP2 scenarios, the farmland and grassland areas were shown to be the smallest in the SSP5 scenario, while the amount of other land use was the biggest. This phenomenon could be attributed to the swift proliferation of urban development, leading to significant encroachment into arable land and grassland areas. Furthermore, according to the SSP5 scenario, the significant growth in the economy resulted in a substantial rise in the amount of woodland and construction land, making them the two types of land with the fastest expansion. The magnitude of the overall change under SSP5 is greater than that under SSP1 and SSP2, as shown in Figures 7 and 8. This is precisely consistent with the research findings of Fan's land cover change simulation in the BTH region, which was conducted using several scenarios of SSP-RCP [35].

3.4. Habitat Quality Prediction Based on SSPs Scenarios

The average habitat quality within a 30 m × 30 m grid was calculated based on the spatial distribution map of habitat quality obtained from the InVEST model for the time period spanning from 2000 to 2050 (as depicted in Figures 5 and 10). This calculation is illustrated in Figure 11. The findings of the study indicate that there was a discernible improvement in the habitat quality within the designated study area over the period spanning from 2000 to 2010. Notably, this positive trend exhibited the highest rate of increase observed throughout the entire duration of the study, amounting to a substantial 2.40%. During the period from 2010 to 2020, an observable pattern emerged wherein the quality of the habitat experienced a discernible decline, characterized by a reduction of 0.27%. Within the timeframe spanning from 2020 to 2050, an analysis conducted under the SSP1 scenario revealed a discernible pattern in the mean habitat quality. Specifically, this pattern exhibited a sequence of declining, rising, and subsequently declining trends. In the context of the SSP2 scenario, it is observed that the mean habitat quality exhibited a pattern characterized by an initial increase, followed by a subsequent decrease, and finally another increase. Conversely, under the SSP5 scenario, the mean habitat quality displayed a consistent and uninterrupted upward trend. In comparison to the year 2020, it is observed that the average habitat quality across the three scenarios in the year 2050 will exhibit an overall increase. Notably, the scenario known as SSP5 will experience the most substantial increase, with a rise of 0.60%. The observed data reveal that SSP1 exhibited the most modest growth, with a marginal increment of merely 0.23%. The second scenario, referred to as SSP2, exhibits a concentration level of 0.42 percent.

The data regarding habitat quality in 2050 and 2020, under various scenarios, were overlaid in ArcGIS. This allowed for the determination of the spatial distribution of changes in the habitat quality area (Figure 12) and changes in the habitat quality grade (Figure 13). The findings revealed that the optimal grade area constituted the smallest percentage (26.91%) in the SSP1 scenario and the maximum percentage (27.10%) in the SSP5 scenario. In the SSP1 scenario, the medium-grade area occupies the largest proportion at 14.88%, while in the SSP5 scenario, it represents the least proportion at 14.70%. The extent of low- to medium-quality habitat was consistent between the SSP1 and SSP2 scenarios. SSP1, SSP2, and SSP5 exhibited a predominant transition of habitat quality from a reasonably high grade to high grade, measuring 420.27 km², 492.65 km², and 552.79 km², respectively. The reduction in the habitat quality grade was primarily observed in Lingqiu County, Fuping County, Quyang County, Tang County, Shunping County, Mancheng District, and Fangshan District. These locations exhibited a cross-hook distribution pattern. The areas exhibiting superior habitat quality are primarily Fuping County and Laishui County, situated on both sides of the connection, as well as BYD District.

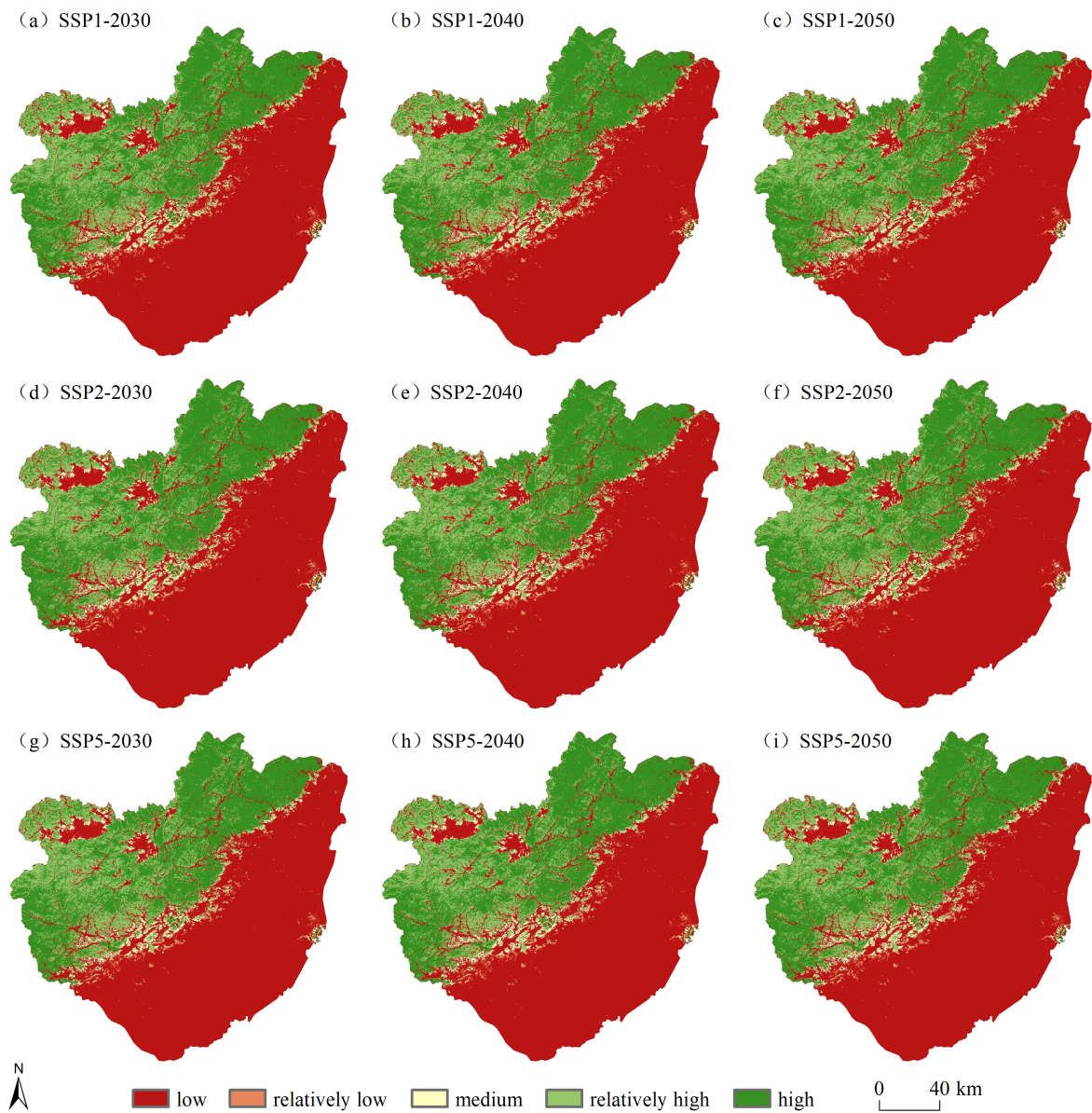


Figure 10. Habitat quality of BYD basin in 2030, 2040, and 2050 under different scenarios.

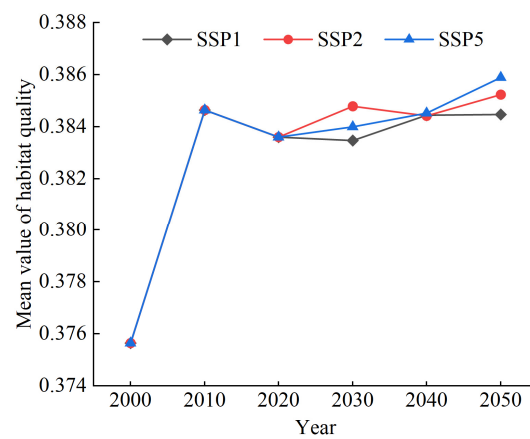


Figure 11. Change of mean value of habitat quality in BYD Basin from 2000 to 2050.

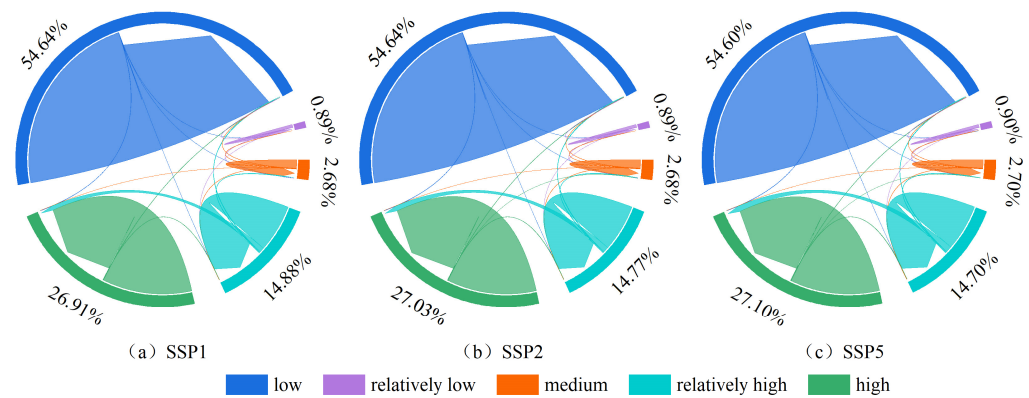


Figure 12. Habitat quality transfer in BYD Basin under different SSPs scenarios from 2020 to 2050.

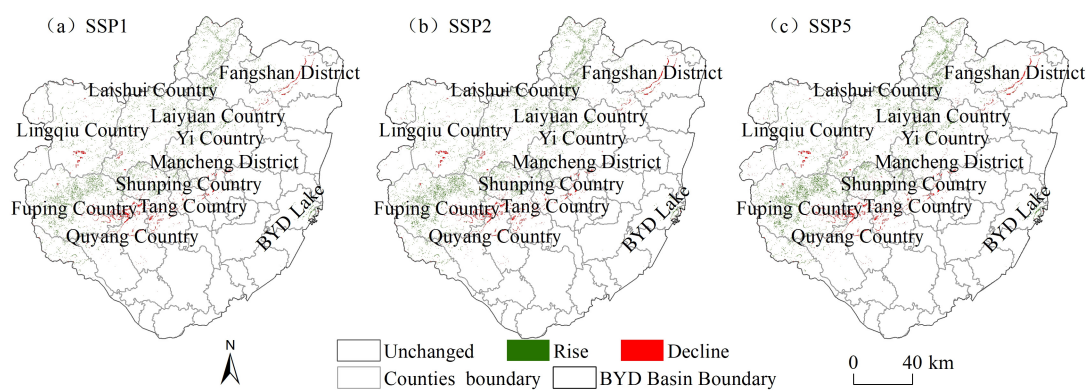


Figure 13. Changes of habitat quality grade in BYD Basin under different SSPs scenarios from 2020 to 2050.

4. Discussion

4.1. Land Use Change Driving Mechanisms

Based on the forecasting results, it is evident that LUCC under the three scenarios is significantly influenced by regional policies and ecological investments. The overall trends indicate an increase in areas designated for construction, woodland, and water bodies, while the extent of cropland and grassland gradually diminishes. Since the year 1980, the implementation of national afforestation initiatives, namely the “Taihang Mountain Greening”, “Sanbei Shelter Forest”, and “Mine Greening Project”, has resulted in a heightened focus on ecological engineering construction. This intensified investment has consequently facilitated substantial growth in the Woodland area within the designated study area, particularly in areas directly visible from Baoding’s 332 and 335 provincial roads. The decrease in grassland area is subject to the influence of economic development and regional policies [36]. One aspect to consider is the extensive conversion of grasslands into arable land, primarily driven by the cultivation of cash crops as a means to augment financial gains. Conversely, it is noteworthy that governmental efforts have been fervently directed towards the restoration of mountainous regions, with a particular emphasis on the conversion of grasslands into woodland areas. Water bodies have experienced significant impacts as a result of water replenishment efforts. Since the establishment of the Xiongan New Area, the area of BYD has experienced a stabilization in its transformation, primarily attributed to the implementation of a systematic mechanism for ecological water replenishment. Economic, demographic, and urbanization factors exert a significant influence on both farmland and construction land. The phenomenon of rapid urbanization, driven by factors such as robust economic growth, population growth, and the migration of rural inhabitants to urban areas, has resulted in the extensive expansion of urban construction land. Consequently, a significant portion of agricultural land has been converted for the purposes

of residential housing, transportation infrastructure, industrial and mining activities, as well as the development of tourist destinations [37,38].

4.2. Causes Analysis of Habitat Quality

A robust correlation exists between habitat quality and the spatial arrangement of land use. The regions of relatively low habitat quality include farmland and construction land [39], characterized by a lower elevation, a higher urbanization degree, and greater susceptibility to human activities. The regions with excellent habitat quality consist of woodland and water areas, whereas the regions with somewhat high habitat quality are primarily found in grasslands. The location with high and relatively high habitat quality exhibits more elevation, a comparatively lower urbanization degree, and is less impacted by human activity. The rapid growth of urban areas and the high concentration of people have altered the land use types, which has led to the disruption of the structure and functioning of ecosystems, primarily seen in the reduction of woodland, grassland, and farmland areas, as well as an increase in fragmentation [40,41]. The significant improvement in habitat quality during the period from 2000 to 2010 can be attributed to the rise in woodland area. During this time frame, while the amount of land used for construction increased, the majority of this growth occurred in the plains and had minimal influence on the overall quality of the basin's ecosystem. The primary factors contributing to the reduction in habitat quality from 2010 to 2020 are the expansion of construction land into farmland in mountainous regions and the encroachment of farmland into grassland in mountainous areas. Throughout the specified time frame, while the expansion of woodland positively impacted the quality of habitat in certain regions, there was a noticeable increase in construction land and farmland in the mountainous area. As a consequence, the overall habitat quality in the basin decreased compared to the period from 2000 to 2010.

In contrast to the conclusions drawn by most scholars, the habitat quality in the BYD basin has shown an increase under the scenarios of SSP1, SSP2, and SSP5, with the highest improvement observed under SSP5. This variation may be attributed to the topography and land changes in the BYD basin, which is generally divided by a southwest-northeast diagonal line. The western region consists of mountainous areas, characterized by predominant land use types such as woodland and grassland. In contrast, the eastern region is a plain area where the primary land use types are cropland and construction land. As the urbanization process advances, the increase in construction land primarily results from the conversion of cropland in the eastern plains, thereby having minimal impact on habitat quality. Simultaneously, with increased ecological water replenishment in the BYD lake and augmented investments in the development of western woodland, the areas covered by these two land use types have expanded rapidly. This overall trend contributes to an enhancement in the habitat quality of the BYD basin.

4.3. Uncertainties and Implications

Future research work and uncertainties: The parameter setting of the InVEST model primarily relies on the existing literature and expert assessment, thus exhibiting a certain degree of subjectivity. Further investigation is required in order to adequately quantify the sensitivity of LUCC types to various threat factors. Furthermore, it is imperative to acknowledge that the future LUCC is intricately influenced by a multitude of factors, including but not limited to economic development, national policies, and the climate environment. Furthermore, urban expansion is a highly intricate process characterized by significant uncertainty and complexity. The relationship among the population, economy, and urban land area is not simply a straightforward linear correlation [42]. However, it is crucial to acknowledge that the simulation outcomes of every scenario retain significant reference value in assessing the impact of LUCC on habitat quality. The findings of this study serve as a scientific basis for informing the development of pertinent regional policies. The maintenance of regional ecological security holds immense significance.

5. Conclusions

This paper presents a comprehensive framework system for forecasting land use and habitat quality, drawing upon the SD, PLUS, and InVEST models. The framework is designed to analyze and discuss the evolution trend of spatio-temporal patterns from 2000 to 2050 under various SSP scenarios. By utilizing these models, the study aims to provide valuable insights into the future dynamics of land use and habitat quality. The primary findings are outlined below:

From 2000 to 2020 and from 2020 to 2050, the Baiyangdian watershed experienced a decreasing trend in the areas of cultivated land, grassland, and unused land, while forest land and construction land exhibited an increasing trend. The primary transitions in land use types were from cultivated land to construction land and from grassland to forest land. Habitat quality showed a high consistency with the spatial distribution of land use. Good and excellent habitat quality levels were mainly concentrated in the northwest mountainous region dominated by grassland and forest land. Poor quality was primarily distributed in the southeast plain area dominated by cultivated land and construction land, while fair and poor levels were interspersed in the transitional zone between mountains and plains. The overall magnitude of changes in land use types under the SSP5 scenario was higher than that under the SSP1 and SSP2 scenarios. Habitat quality level transitions were mainly from good to excellent. In comparison to the year 2020, habitat quality increased in 2050 under all three scenarios, with the highest increase observed in SSP5 and the smallest increase in SSP1.

Author Contributions: Writing—original draft preparation, Z.H. (Zhen Han) and B.L.; writing—review and editing, S.W. and Z.H. (Zepeng Han); methodology, W.P., X.L. and D.B.; visualization, Z.H. (Zhen Han) and B.L.; data curation, B.L. All authors have read and agreed to the published version of the manuscript.

Funding: This research was funded by the Independent research project of State Key Laboratory of Simulation and Regulation of Water Cycle in River Basin (NO. SKL2022ZD02), the Basic Scientific Research Expense Project of IWHR (WE110145B0012023).

Data Availability Statement: The data have been explained in the paper.

Conflicts of Interest: The authors declare no conflicts of interest.

References

1. Zhong, L.N.; Wang, J. Assessing the impact of land consolidation on habitat quality based on InVEST model. *Trans. Chin. Soc. Agric. Eng.* **2017**, *33*, 250–255.
2. Fellman, J.B.; Hood, E.; Dryer, W.; Pyare, S. Stream Physical Characteristics Impact Habitat Quality for Pacific Salmon in Two Temperate Coastal Basins. *PLoS ONE* **2015**, *10*, e0132652. [[CrossRef](#)]
3. Wu, J.S.; Cao, Q.W.; Shi, S.Q.; Huang, X.L.; Lu, Z.Q. Spatiotemporal evolution of habitat quality in Beijing-Tianjin-Hebei based on land use change. *Chin. J. Appl. Ecol.* **2015**, *26*, 3457–3466.
4. Newbold, T.; Hudson, L.N.; Hill, S.L.L.; Contu, S.; Lysenko, I.; Senior, R.A.; Brger, L.; Bennett, D.J.; Choimes, A.; Collen, B.; et al. Global effects of land use on local terrestrial biodiversity. *Nature* **2015**, *520*, 45–50. [[CrossRef](#)] [[PubMed](#)]
5. Wu, L.N.; Yang, S.T.; Liu, X.Y.; Luo Ya Zhou, X.; Zhao, H.G. Response of land use change to human activity in Beiluo River Basin since 1976. *Acta Geogr. Sin.* **2014**, *69*, 54–63.
6. Zhang, X.R.; Zhou, J.; Li, M.M. Spatial and temporal variation of regional habitat quality based on land use pattern reconstruction. *Acta Geogr. Sin.* **2020**, *75*, 160–178.
7. Kang, J.; Fang, L.; Li, S.; Wang, X. Parallel Cellular Automata Markov Model for Land Use Change Prediction over MapReduce Framework. *ISPRS Int. J. Geo-Inf.* **2019**, *8*, 454. [[CrossRef](#)]
8. Shirmohammadi, B.; Malekian, A.; Salajegheh, A.; Taheri, A.; Azarnivand, H.; Malek, Z.; Verburg, P.H. Scenario analysis for integrated water resources management under future land use change in the Urmia Lake region, Iran. *Land Use Policy* **2020**, *90*, 104299. [[CrossRef](#)]
9. Liu, X.P.; Liang, X.; Li, X.; Li, X.; Xu, X.C.; Ou, J.P.; Chen, Y.M.; LIS, Y.; Wang, S.J.; Pei, F.S. A future land use simulation model (FLUS) for simulating multiple land use scenarios by coupling human and natural effects. *Landsc. Urban Plan.* **2017**, *168*, 94–116. [[CrossRef](#)]
10. Zhang, S.; Zhong, Q.; Cheng, D.; Xu, C.; Chang, Y.; Lin, Y.; Li, B. Landscape ecological risk projection based on the PLUS model under the localized shared socioeconomic pathways in the Fujian Delta region. *Ecol. Indic.* **2022**, *136*, 108642. [[CrossRef](#)]

11. Lin, Q. Dynamic simulation of land use change and assessment of carbon storage based on climate change scenarios at the city level: A case study of Bortala, China. *Ecol. Indic.* **2022**, *134*, 108499.
12. He, C.Y.; Shi, P.J.; Li, J.G.; Pan, Y.Z.; Chen, J. Scenario simulation of future land use change in northern China. *Acta Geogr. Sin.* **2004**, *59*, 599–607.
13. Jiang, X.F.; Duan, H.C.; Liao, J.; Song, X.; Xue, X. Land use in Ganlingao area of Middle Heihe River Basin based on PLUS-SD coupling model. *J. Arid Zone Res.* **2022**, *4*, 1246–1258.
14. Liang, X.; Guan, Q.F.; Clarke, K.C.; Liu, S.S.; Wang, B.Y.; Yao, Y. Understanding the drivers of sustainable land expansion using a patch-generating land use simulation (PLUS) model: A case study in Wuhan, China. *Comput. Environ. Urban Syst.* **2021**, *85*, 101569. [[CrossRef](#)]
15. Wang, J.; Zhang, J.; Xiong, N.; Liang, B.; Wang, Z.; Cressey, E.L. Spatial and Temporal Variation, Simulation and Prediction of Land Use in Ecological Conservation Area of Western Beijing. *Remote Sens.* **2022**, *14*, 1452. [[CrossRef](#)]
16. He, N.; Guo, W.; Wang, H.; Yu, L.; Cheng, S.; Huang, L.; Jiao, X.; Chen, W.; Zhou, H. Temporal and Spatial Variations in Landscape Habitat Quality under Multiple Land-Use/Land-Cover Scenarios Based on the PLUS-InVEST Model in the Yangtze River Basin, China. *Land* **2023**, *12*, 1338. [[CrossRef](#)]
17. Huang, M.Y.; Yue, W.Z.; Feng, S.R.; Zhang, J. Spatial-temporal evolution of habitat quality and analysis of landscape patterns in Dabie Mountain area of west Anhui province based on InVEST model. *Acta Ecol. Sin.* **2020**, *40*, 2895–2906.
18. Sallustio, L.; De Toni, A.; Strollo, A.; Di Febbraro, M.; Gissi, E.; Casella, L.; Geneletti, D.; Munafò, M.; Vizzarri, M.; Marchetti, M. Assessing habitat quality in relation to the spatial distribution of protected areas in Italy. *J. Environ. Manag.* **2017**, *201*, 129–137. [[CrossRef](#)] [[PubMed](#)]
19. Moreira, M.; Fonseca, C.; Vergílio, M.; Calado, H.; Gil, A. Spatial assessment of habitat conservation status in a Macaronesian island based on the InVEST model: A case study of Pico Island (Azores, Portugal). *Land Use Policy* **2018**, *78*, 637–649. [[CrossRef](#)]
20. Li, X.; Liu, Z.; Li, S.; Li, Y. Multi-scenario simulation analysis of land use impacts on habitat quality in Tianjin based on the PLUS model coupled with the InVEST model. *Sustainability* **2022**, *14*, 6923. [[CrossRef](#)]
21. Wang, R.Y.; Zhao, J.S.; Chen, G.P.; Lin, Y.L.; Yang, A.R.; Chen, J.Q. Coupling PLUS-InVEST Model for Ecosystem Service Research in Yunnan Province, China. *Sustainability* **2023**, *15*, 271. [[CrossRef](#)]
22. Babbar, D.; Areendran, G.; Sahana, M.; Sarma, K.; Raj, K.; Sivadas, A. Assessment and prediction of carbon sequestration using Markov chain and InVEST model in Sariska Tiger Reserve, India. *J. Clean. Prod.* **2021**, *278*, 123333. [[CrossRef](#)]
23. Jing, C.; Jiang, T.; Su, B.D.; Wang, G.J.; Luo, Y.; Zhai, J.Q.; Huang, J.L.; Jing, C.; Gao, M.N.; Lin, Q.G.; et al. Application of shared socioeconomic pathways in land use, energy and carbon emission research. *Chin. J. Atmos. Sci.* **2022**, *45*, 397–413.
24. Jiang, T.; Su, B.D.; Wang, Y.J.; Wang, R.; Zhao, J.; Jing, C.; Cao, L.G.; Sun, H.M.; Wang, A.Q.; Huang, J.L. Shared Socioeconomic Pathways (SSPs) population and Economy lattice dataset. *Adv. Clim. Chang. Res.* **2022**, *18*, 381–383.
25. Tang, Q.; Yu, P.H.; Chen, Z.Y.; Bai, S.Y.; Chen, Y.Y. Simulation of land use change under shared socioeconomic path. *Res. Soil Water Conserv.* **2022**, *29*, 301–310.
26. Meiyappan, P.; Dalton, M.; O’Neill, B.C.; Jain, A.K. Spatial modeling of agricultural land use change at global scale. *Ecol. Model.* **2014**, *291*, 152–174. [[CrossRef](#)]
27. Ma, Z.; Wang, W.; Hou, X.; Wang, J.; Duan, L.; Wang, Y.; Zhao, M.; Li, J.; Jing, J.; Li, L. Examining the change in groundwater flow patterns: A case study from the plain area of the Baiyangdian Lake Basin, North China. *J. Hydrol.* **2023**, *625*, 130160. [[CrossRef](#)]
28. Cai, Y.; Zhang, P.; Wang, Q.; Wu, Y.; Ding, Y.; Nabi, M.; Fu, C.; Wang, H. How does water diversion affect land use change and ecosystem service: A case study of Baiyangdian wetland, China. *J. Environ. Manag.* **2023**, *344*, 118558. [[CrossRef](#)]
29. Yang, J.; Huang, X. The 30 m annual land cover dataset and its dynamics in China from 1990 to 2019. *Earth Syst. Sci. Data* **2021**, *13*, 3907–3925. [[CrossRef](#)]
30. Li, F.X.; Liu, D.F.; Kong, X.S.; Liu, Y.L. Multi-scenario county sustainable development potential evaluation based on dynamic simulation perspective and shared socio-economic path. *J. Geoinf. Sci.* **2022**, *24*, 684–697.
31. Sharp, R. Natural Capital Project. In *InVEST 3.14.1 User’s Guide*; Stanford University, University of Minnesota, Chinese Academy of Sciences, The Nature Conservancy, World Wildlife Fund, and Stockholm Resilience Centre: Morges, Switzerland, 2022.
32. Liao, Z.M.; Yang, W.; CAIX, P.; Wang, X.; Xiong, W.S. Ecological function evaluation and zoning of Daqinghe-Baiyangdian Basin. *Chin. J. Environ. Sci.* **2022**, *42*, 131–140.
33. Zhang, D.Z.; Sun, X.Y.; Yuan, X.Z.; Liu, F.; Guo, H.W.; Xu, Y.; Li, B.F. Land use change and its impact on habitat quality in Nansi Lake Basin, 1980–2015. *J. Lake Sci.* **2018**, *30*, 349–357.
34. He, J.; Huang, J.; Li, C. The evaluation for the impact of land use change on habitat quality: A joint contribution of cellular automata scenario simulation and habitat quality assessment model. *Ecol. Model.* **2017**, *366*, 58–67. [[CrossRef](#)]
35. Fan, Z.M. Simulation of land cover change in Beijing-Tianjin-Hebei region based on different scenarios of SSP-RCP. *Acta Geogr. Sin.* **2022**, *77*, 228–244.
36. Xu, Z.T.; Chen, P.F.; Zhou, S.J.; Zhu, Y.Q.; Shi, Y.J. Land cover change and its ecological service value evaluation in Baiyangdian Basin. *Ecol. Sci.* **2018**, *37*, 83–90.
37. Wen, J.; Huang, D.Z. Spatial and temporal variation of landscape structure and pattern in Baiyangdian Basin and its relationship with topographic factors. *J. Agric. Univ. Hebei* **2020**, *43*, 86–95.
38. Zhang, M.Y.; Wang, K.L.; He, P.; Xie, Z.R.; Gao, J.X. Study on landscape spatial pattern change in Baiyangdian Basin. *Resour. Sci.* **2005**, *27*, 134–140.

39. Wang, J.; YANY, L.; Wang, J.M.; Ying, L.X.; Tang, Q. Spatial and temporal characteristics and prediction of habitat quality in Minjiang River Basin. *Acta Ecol. Sin.* **2021**, *41*, 5837–5848.
40. Guo, M.; Shu, S.; Ma, S.; Wang, L.J. Using high-resolution remote sensing images to explore the spatial relationship between landscape patterns and ecosystem service values in regions of urbanization. *Environ. Sci. Pollut. Res.* **2021**, *28*, 56139–56151. [[CrossRef](#)] [[PubMed](#)]
41. Zhang, X.M.; Wang, J.; Yue, C.L.; Ma, S.; Wang, L.J. Exploring the spatiotemporal changes in carbon storage under different development scenarios in Jiangsu Province, China. *PeerJ* **2022**, *10*, e13411. [[CrossRef](#)] [[PubMed](#)]
42. Chen, X.; Zhang, H.; Chen, W.; Huang, G. Urbanization and climate change impacts on future flood risk in the Pearl River Delta under shared socioeconomic pathways. *Sci. Total Environ.* **2021**, *762*, 143144. [[CrossRef](#)] [[PubMed](#)]

Disclaimer/Publisher’s Note: The statements, opinions and data contained in all publications are solely those of the individual author(s) and contributor(s) and not of MDPI and/or the editor(s). MDPI and/or the editor(s) disclaim responsibility for any injury to people or property resulting from any ideas, methods, instructions or products referred to in the content.